



Disclosing the distinct interfacial behaviors of structurally and configurationally diverse triazologlycolipids

Xiao-Peng He, Xiaolian Xu, Hai-Lin Zhang, Guo-Rong Chen*, Shouhong Xu*, Honglai Liu

Key Laboratory for Advanced Materials and Institute of Fine Chemicals, East China University of Science and Technology, 130 Meilong Road, Shanghai 200237, PR China

ARTICLE INFO

Article history:

Received 10 February 2011

Received in revised form 8 April 2011

Accepted 26 April 2011

Available online 3 May 2011

Keywords:

Glycolipid

Click chemistry

LB film

Atomic force microscopy

π -A isotherm

ABSTRACT

1- or 6-Triazologluco- and galactolipid derivatives bearing a lipid chain length of 16 carbons were efficiently constructed via click chemistry. The differentiation in their surface pressure-molecular area (π -A) isotherms first implies that these structurally and configurationally diverse amphiphiles adopt different distribution manner at air-water interfaces. The Langmuir-Blodgett (LB) films of the synthesized glycoconjugates on mica surface were subsequently prepared and visualized via atomic force microscopy (AFM), which exhibited diverse topographies and possess different contact angles with water. These data further suggest that the structural variation as well as epimeric identity of triazologlycolipids may result in their distinct interfacial behaviors at the air-solid interface. Furthermore, the addition of increasing amounts of 1-triazogalactolipid 2 to poly-diacetylene (PDA) was determined to impact the π -A isotherm of the latter, prompting us to further fabricate new colorimetrically detectable mixed-type vesicles containing triazologlycolipids for biochemical studies.

© 2011 Elsevier Ltd. All rights reserved.

1. Introduction

Glycolipids universally distribute in nature, constituting cell membranes of almost all living organisms. They are widely applicable in numerous biochemical and especially physicochemical studies owing to their intrinsic amphiphilic feature as well as their low toxicity and high biocompatibility.^{1–11} However, the majority of natural glycolipids encounter unsatisfactory limitations such as their structural instability toward acidic and enzymatic cleavage due to the presence of an O-glycosidic linkage between the lipid aglycons and the glycons.

The regioselective and high-yielding Cu(I)-catalyzed alkyne-azide 1,3-dipolar cycloaddition (a representative of click chemistry¹²), which was first defined by Sharpless and co-workers has emerged as a versatile tool¹³ that enables the diversification of various structurally-stable glycoconjugates with rigid triazole-linkages for multiple practical uses.^{14–28} Nevertheless, the preparation of triazole-linked glycolipids and the disclosure of their potential functions have been relatively rarely reported.^{29–32}

Loganathan and Paul first described the synthesis of series of triazologlycolipid mimetics in which the triazole ring serves as a solid connection between various carbohydrates and lipid chains.²⁹ Krausz and co-workers subsequently showed the potential utility of this unique non-ionic lipid class for the development of green

surfactants.³⁰ In addition, the surface characterizations of these functional natural analogs were recently reported by Auzanneau and co-workers,³¹ and us, independently.³²

With a continued interest in the further exploration with regard to the use of triazole-functionalized glycolipids, we describe here their interesting interfacial behaviors. Structurally and configurationally diversified triazologluco- and galactolipids bearing a 16 carbon lipid chain were efficiently prepared via click chemistry. The apparent differentiations in their π -A isotherms and LB film characteristics on mica indicate that both the substitution position of the lipid chain and the epimeric identity on carbohydrate moiety significantly influences the interfacial properties of the produced triazologlycolipids. Moreover, the π -A isotherm of PDA was then determined to be variable in the presence of the 1-triazogalactolipid, prompting further fabrication of mixed-type vesicles colorimetrically detectable for carbohydrate-related biochemical investigations.

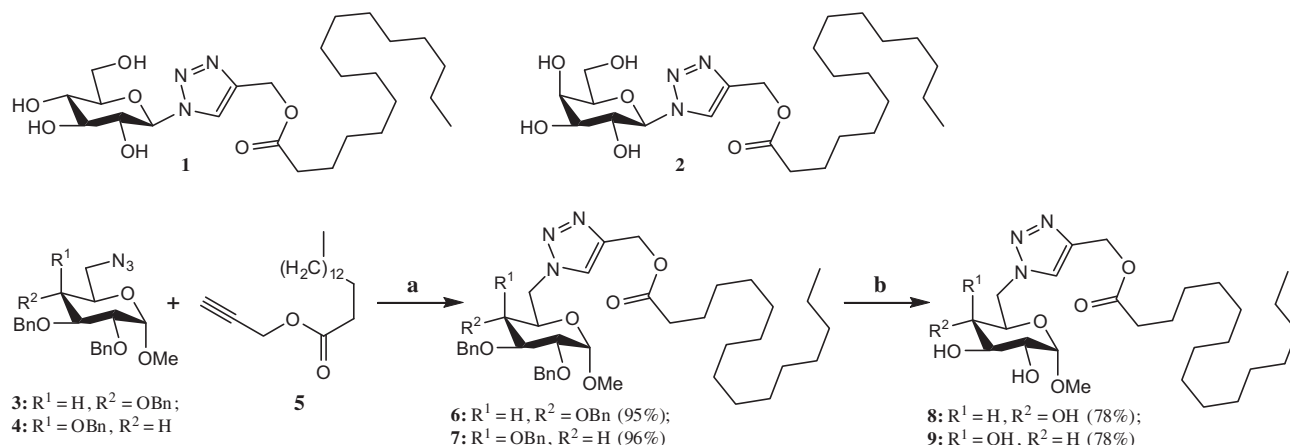
2. Results and discussion

2.1. Preparation of triazologlycolipids

1-Distributed natural glycolipid triazoloanalogs **1** and **2** (Scheme 1) were prepared previously, and were shown to have promising adsorption ability on gold-surfaces.³² For the evaluation of structure-interfacial activity relationship (SAR), 6-distributed triazoles **8** and **9** were synthesized. The known methyl 6-azido-6-deoxy- α -D-glucopyranoside and galactopyranoside, **3** and **4**,

* Corresponding authors. Tel.: +86 21 64251942; fax: +86 21 64252921.

E-mail addresses: mrs_guorongchen@ecust.edu.cn (G.-R. Chen), xushouhong@ecust.edu.cn (S. Xu).



Scheme 1. Reagents and conditions: (a) Na ascorbate, CuSO₄·5H₂O, CH₂Cl₂/water, rt; (b) PdCl₂/H₂, MeOH, rt.

were previously prepared^{33,34} while the lipid alkyne **5** was readily synthesized from commercially available palmitic acid in the presence of 1.5 equiv K₂CO₃ and propargyl bromide in anhydrous DMF.

The click reaction of azide **3** and **4** with the alkyne **5** proceeded with the promotion of Na ascorbate and CuSO₄·5H₂O in CH₂Cl₂–water (1:1, v/v) at rt, shown in Scheme 1. To our delight, the two click adducts, **6** and **7**, were afforded smoothly in excellent yields of 95% and 96%, respectively. Subsequent hydrogenolysis catalyzed by a reported PdCl₂–H₂ system (in MeOH)³² furnished the desired triazolgluco- (**8**) and galactolipid (**9**) in good yield of 78%. All new compounds (**6**–**9**) were structurally confirmed by NMR and HRMS.

2.2. Study of interfacial properties

2.2.1. π - A isotherms of triazolglycolipids monolayers

The π - A isotherms of various glycolipids (**1**, **2**, **8** and **9**) monolayers were first measured, which displayed similar shapes without characteristic transitions (Fig. 1). The π - κ curves, obtained by plotting various surface pressures as a function of their calculated κ (compressibility) values (equation indicated in the Supplementary data) were then prepared (Fig. S-1, Supplementary data). All κ values of these monolayers are in the range of 0.018–0.060 m/mN, revealing that they would be most likely in the liquid expanded phase.^{35–42}

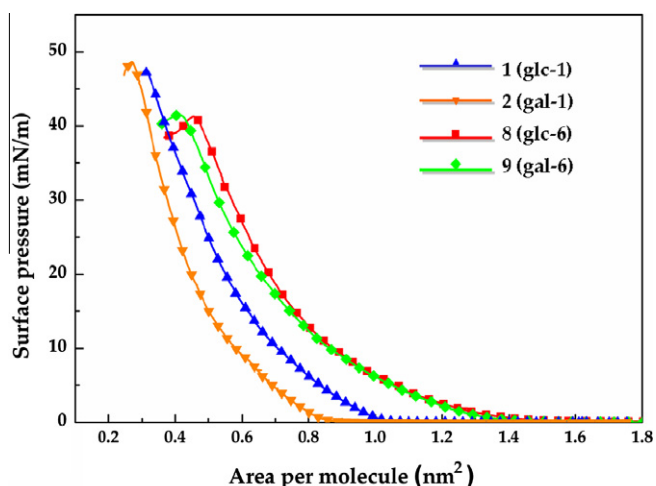


Figure 1. The π - A isotherms of various triazolglycolipid monolayers. The curves represent those of compounds **2** (gal-1), **1** (glc-1), **9** (gal-6) and **8** (glc-6), respectively, from left to right.

Table 1

The values of A_L and π_c of the glycolipids **1**, **2**, **8** and **9**

Compound	A_L (nm ²)	π_c (mN/m)
1	1.04	47.3
2	0.86	48.6
8	1.50	40.4
9	1.41	41.3

As shown in Table 1, the liftoff areas (A_L , the molecular occupation area where the isotherm rises just from the baseline)³⁵ of 1-substituted compounds (1.04 nm² for **1** and 0.86 nm² for **2**) are around 1.5-fold smaller than those of their 6-substituted counterparts (1.50 nm² for **1** and 1.41 nm² for **2**), indicating that the 6-triazolglycolipids distribute less tightly on the air–water interface than the 1-triazolglycolipids. The collapse pressures (π_c) of each triazolglycolipid monolayer were also obtained from Figure 1 and are summarized in Table 1. The π_c values of 6-triazolglycolipid monolayers (around 41 mN/m) are smaller than those of 1-triazolglycolipid ones (around 48 mN/m), demonstrating that the latter is more stable than the former at gas–liquid interface.

In addition, the A_L value of 1-distributed galactolipid **2** (0.86 nm²) is smaller than that of the glucolipid **1** (1.04 nm²), which means that the former bearing a C4 axial hydroxyl bond may occupy lesser space on the air–water interface compared to that of the latter, which has an equatorial hydroxyl bond at C4. However, we observed that the difference in A_L value between 6-distributed galactolipid **9** (1.41 nm²) and glucolipid **8** (1.50 nm²) is much smaller than that between the 6-distributed derivatives (**8** and **9**). This could be most likely ascribed to the existence of C6-triazololipid on glycoside **8** and **9**, which is spatially much closer to the C4-OH of the monosaccharide moiety compared to the C1-triazololipid on compound **1** and **2**, furnishing excess steric hindrance that reduces the C4-epimeric effect of carbohydrates toward the interfacial property of the corresponding amphiphiles.

2.2.2. LB films of triazolglycolipids

To investigate their interfacial properties in a more detailed way, the LB films of the four synthesized compounds (**1**, **2**, **8** and **9**) under various surface pressures (5, 15, 25 and 35 mN/m) were prepared on mica surface and their AFM images were obtained and shown in Figure 2 (only the results of π equals to the lowest 5 mN/m and the highest 35 mN/m were displayed for a clearer comparison). Cross sections of the AFM images obtained by off-line analysis software were also shown while the hydrophobicity of these films was studied via the water contact angles θ , summarized in Table 2.

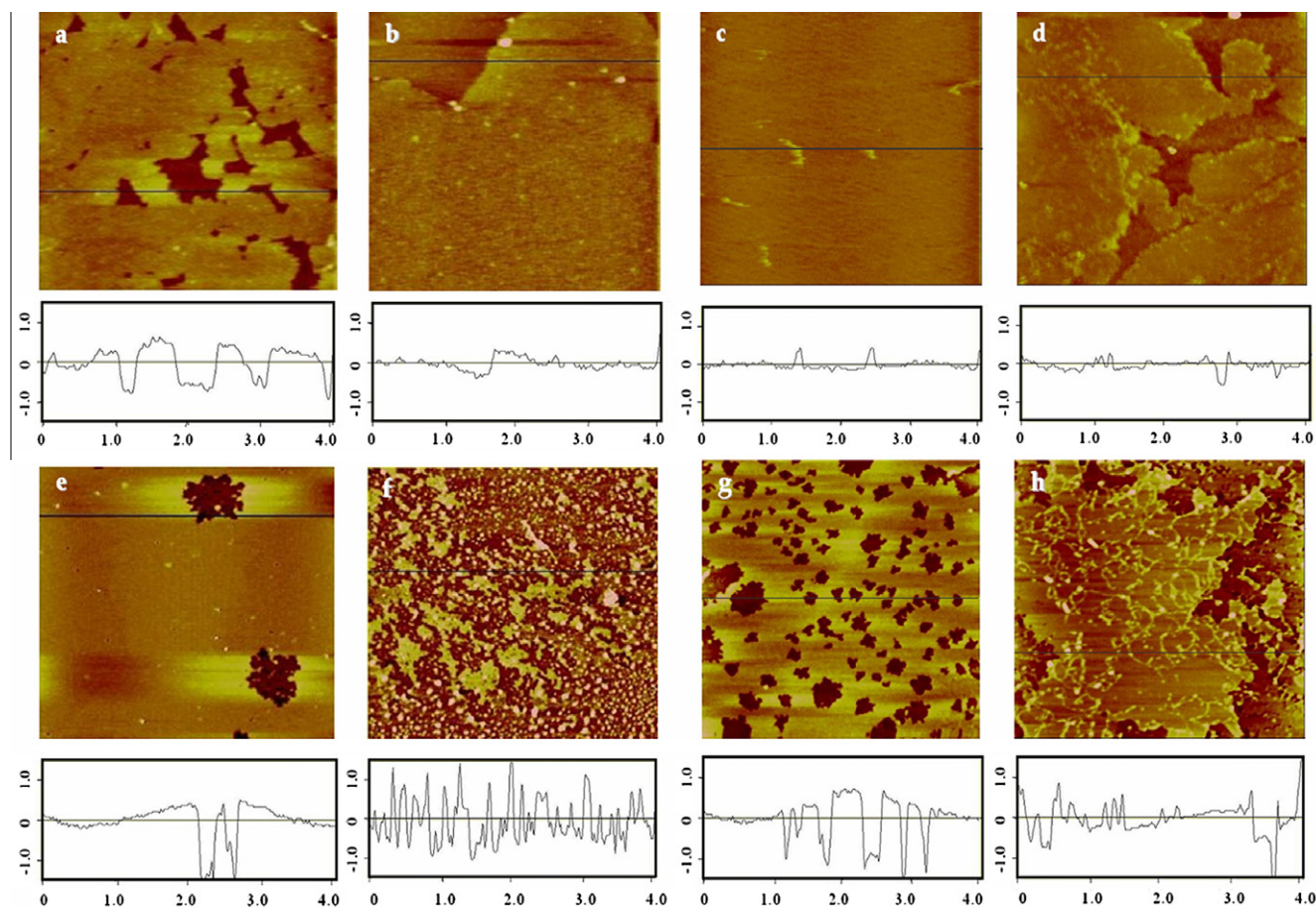


Figure 2. AFM images ($4 \times 4 \mu\text{m}$) of (a) compound **1**, $\pi = 5 \text{ mN/m}$; (b) compound **1**, $\pi = 35 \text{ mN/m}$; (c) compound **2**, $\pi = 5 \text{ mN/m}$; (d) compound **2**, $\pi = 35 \text{ mN/m}$; (e) compound **8**, $\pi = 5 \text{ mN/m}$; (f) compound **8**, $\pi = 35 \text{ mN/m}$; (g) compound **9**, $\pi = 5 \text{ mN/m}$; (h) compound **9**, $\pi = 35 \text{ mN/m}$. Cross sections obtained along the black lines in AFM topographic images a–h are also shown underneath (abscissa: 0–4.0 μm ; ordinate: –0.1 to 0.1 nm).

Clearly, the AFM topographies between the 1-substituted (Fig. 2a–d) and 6-substituted (Fig. 2e–g) triazologlycolipids appeared to be distinct under both low and high surface pressures. As shown in Figure 2a, a low and gapped platform of 1-triazologlycolipid **1** having a terrace of 0.5 nm in height was formed at $\pi = 5 \text{ mN/m}$ whereas such a platform tended to become an integrated and thicker molecular layer when the surface pressure increased to 35 mN/m (Fig. 2b). In contrast, the LB film of 1-triazologlycolipid **2** (Fig. 2c) was initially more compactly formed on mica at $\pi = 5 \text{ mN/m}$ compared to that of its epimer **1** (Fig. 2a). With successively increased pressure (35 mN/m), this film was structurally tightened and thickened as shown in Figure 2d similar to the topographical change of the LB film containing compound **1** from Figure 2a and b.

Nevertheless, the topographies of the LB films formed by the 6-triazologlycolipids are dissimilar under different pressures. Pits of about 2 nm in depth were observed in the LB film of 6-triazologlycolipid **8** (Fig. 2e, $\pi = 5 \text{ mN/m}$), which then disappeared with

increased surface pressure ($\pi = 35 \text{ mN/m}$). Instead, some small terraces with less than 1 nm in height were observed (Fig. 2f) right on the originally formed molecular film. Likewise, the LB film of 6-triazologlycolipid **9** with widely distributed pits of about 2 nm was previously formed on mica under the pressure of 5 mN/m (Fig. 2g), whereas increased pressure (35 mN/m) led to the similar formation of even more densely functionalized terraces with height of less than 1 nm, displayed in Figure 2h.

Interestingly, the 6-triazologlycolipids may constitute thicker LB films compared to their 1-triazologlycolipids counterparts under low surface pressure. When the pressure increased, the LB films of the latter tended to become more compact and thicker whereas additional terraces appeared on that of the former. In an attempt to propose an explanation toward such phenomenon, the plausible morphological changes of LB films containing the 6- or 1-triazologlycolipids from air–water interface to mica surface were illustrated in Figure 3.

We postulate that by pulling up the mica slice from water, the 6-triazologlycolipids attached on mica surface would adopt a standing posture with the lipid end being vertical-like to the surface (Fig. 3b). However, considering the comparatively thinner LB films formed by the 1-triazologlycolipids (around 0.5 nm vs 2.0 nm in thickness of 6-triazologlycolipid films), these molecules would possibly choose to sprawl on the surface as shown in Figure 3a.⁴³ Upon the increase in pressure, the 1-distributed amphiphiles would probably ‘stand up’ with erected lipid chains toward air (Fig. 3c) and distribute more tightly on the mica surface deduced by their observed AFM topographies (Fig. 2b and d). In contrast, with increased pressure, the LB film formed by the initially

Table 2
The θ (water contact angle) values of LB films formed by glycolipids **1**, **2**, **8** and **9**

Compound	θ^a ($^\circ$)			
	$\pi = 5 \text{ mN/m}$	$\pi = 15 \text{ mN/m}$	$\pi = 25 \text{ mN/m}$	$\pi = 35 \text{ mN/m}$
1	15.05	22.13	25.22	31.62
2	25.59	33.93	43.20	55.49
8	22.01	22.62	22.58	22.47
9	19.73	20.11	21.74	22.71

^a Values are means of six experiments.

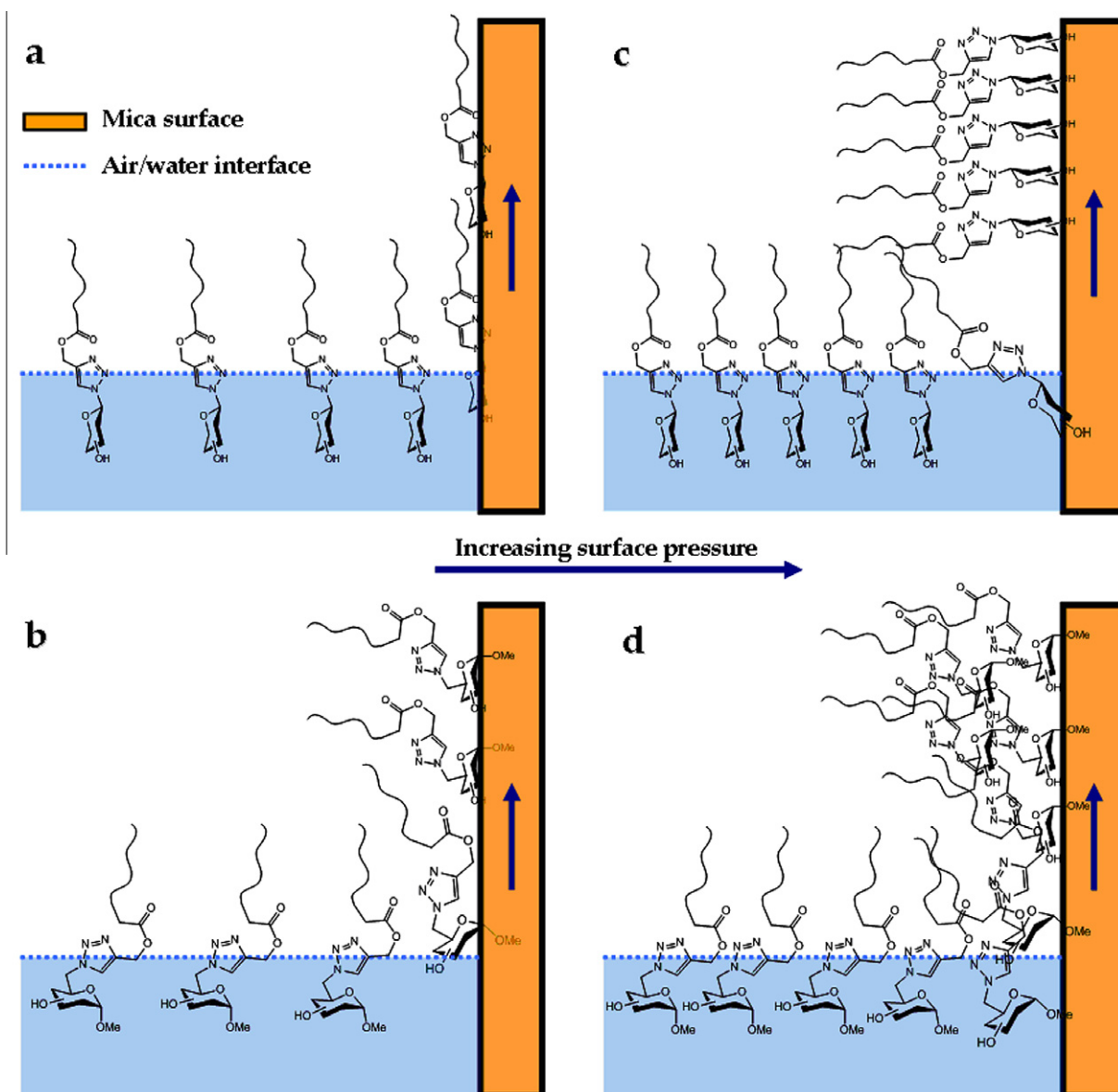


Figure 3. Schematic representation of (a) 1-triazologlycolipid assembly on mica surface under low pressure; (b) 1-triazologlycolipid assembly on mica surface under high pressure, and (c) 6-triazologlycolipid assembly on mica surface under low pressure; (d) 6-triazologlycolipid assembly on mica surface under high pressure.

'stand-up' 6-distributed amphiphiles would be prone to become saturated and the surplus molecules might have been partially extruded from the first layer, illustrated in Figure 3b. We speculate that an overlapped molecular loop instead of a double layer was generated since the height of the additionally emerged terraces observed from Figure 2f and h is less than 1 nm, being onefold smaller in value than that of the bottom film under low pressure (around 2 nm) shown in Figure 2e and g.

As shown in Table 2, at lowest pressure (5 mN/m), the water contact angle (θ) of LB film of 1-triazologlycolipid **1** (15°) is smaller than that of galactolipid **2** (26°), indicating that the LB film formed by the former is less hydrophobic than that formed by the latter. Under gradually increased pressure, the hydrophobicity of both films simultaneously increased with the galactosyl film **2** being always more hydrophilic. However, the water contact angles of 6-triazologlycolipids were determined not to be significantly impacted by both the epimeric effect of monosaccharide moiety and the increasing pressure.

We have previously observed from the π - A isotherms (Fig. 1) of the triazologlycolipid films that the areas occupied by each

molecule of 1-modified galactoside **2** are always apparently smaller than those of its epimer **1** under various surface pressures, which implies that the former could generate tighter molecular films than the latter. Consequently, the more compact monolayer containing compound **2** would be more hydrophobic with larger values in contact angle degree with water. In sharp contrast, the inconspicuous diversity in π - A isotherms between the 6-modified glycosyl epimers (**7** and **8**) suggests their similar molecular film formation, which might successively render their similar θ values. Such similarity between these two molecules could be ascribed to, as described above, the existence of bulky C6-triazololipid moiety spatially contiguous to the glycosyl C4-position, diminishing their epimeric effect on the corresponding interfacial properties.

2.2.3. PDA-triazologlycolipid mixture

Previous reports have supported that the mixture of PDA with natural glycolipids possessing colorimetrically detectable properties may represent a promising strategy for producing vesicles applicable in numerous biochemical studies including sugar-mediated cell-cell recognition, drug release and gene transfection.^{44,45}

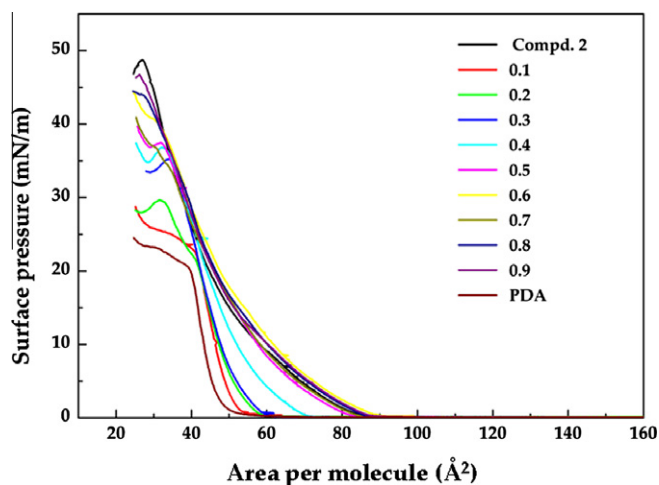


Figure 4. The π - A isotherms of PDA alone, PDA/compound **2** (molar fraction of compd **2**) = 0.1, 0.2, 0.3, 0.4, 0.5, 0.6, 0.7, 0.8, 0.9 and compound **2** alone, respectively, from left to right.

Consequently, the π - A isotherms of PDA–triazologlycolipid mixtures including various molar fractions of the selected 1-triazologalactolipid **2** were preliminarily investigated as shown in Figure 4. The isotherm of the pure PDA is almost linear, which indicates its solid membrane state, whereas the presence of increasing amounts of **2** may gradually lead the corresponding isotherm to liquid state. Moreover, the stability of the membrane formed by the PDA–triazologalactolipid mixture could also be enhanced with the increase of the latter considering their increasing π_c values. These data suggest that the blending of triazologlycolipid with PDA may alter considerably the physicochemical property of the latter, which further prompted us to fabricate a mixed-type vesicle containing these two components for the above-mentioned biochemical studies.

3. Conclusion

In summary, the interfacial behaviors of four 1- and 6-triazologlycolipids synthesized via click chemistry were comparatively studied by evaluating their π - A isotherms at the air–water interface and LB film characteristics on mica surface via AFM technique, and water contact angle measurement. We estimate that such behaviors are largely dependent on both the structural and configurational diversity of these glycoconjugates. Furthermore, the selected 1-triazologalactolipid was found to enhance the stability of pure PDA membrane at water–air interface. This further prompts us to fabricate novel structurally stable triazologlycolipid-containing mixed-type vesicles colorimetrically detectable for biochemical purposes such as the probing of carbohydrate-mediated cell–cell recognition and drug release using carbohydrate as the carrier.

4. Experimental section

4.1. General

All purchased chemicals and reagents are of high commercially available grade. Solvents were purified by standard procedures. All reactions were monitored by TLC (thin-layer chromatography) performed on E-Merck aluminum percolated plates of Silica Gel 60F-254 with detection by UV ($\lambda_{\text{max}} = 254$) or by spraying with 6 N H_2SO_4 and charring at 300 °C. ^1H and ^{13}C NMR spectra were recorded on a Bruker AM-400 spectrometer in CDCl_3 or CD_3OD

solutions using tetramethylsilane as the internal standard (chemical shifts in parts per million). Optical rotations were measured using a Perkin-Elmer 241 polarimeter at room temperature and a 10 cm length cell of a 1 mL volume. Concentrations are given in g/100 mL. Low and high resolution mass spectra were recorded on a Waters LCT Premier XE spectrometer using standard conditions (ESI, 70 eV).

4.2. General procedure for click reaction

To a well-stirred biphasic solution of the sugar azide (1 equiv) and the lipid alkyne (2 equiv) in CH_2Cl_2 (8–10 mL) and H_2O (8 mL), were added $\text{CuSO}_4 \cdot 5\text{H}_2\text{O}$ (3 equiv) and sodium ascorbate (6 equiv) successively. After stirring for 6 h, the resulting mixture was diluted with CH_2Cl_2 (10 mL) and washed with brine (2×5 mL). The combined organic layers were dried over MgSO_4 and then concentrated under reduced pressure to give a crude residue, which was purified by column chromatography.

4.2.1. Methyl 2,3,4-Tri-*O*-benzyl-6-deoxy-6-(1'*H*-1',2',3'-triazolyl-4-yl-hexadecanoate)- α -*D*-glucopyranoside (**6**)

From compound **3** (200 mg, 0.408 mmol) and **5** (240.4 mg, 0.817 mmol), column chromatography (petroleum ether–EtOAc 8:1→3:1) afforded **6** as a white ceraceous solid (303.9 mg, 94.9%). TLC: $R_f = 0.29$ (petroleum ether–EtOAc, 3:1); $[\alpha]_D^{25} +54.9$ (c 0.3, CH_2Cl_2); ^1H NMR (400 MHz, CDCl_3): δ 7.64 (s, 1H), 7.36–7.28 (br m, 15H), 5.19 (dd, $J = 12.8, 20.4$ Hz, 2H), 4.98 (d, $J = 10.7$ Hz, 1H), 4.90 (d, $J = 10.9$ Hz, 1H), 4.81 (d, $J = 10.8$ Hz, 1H), 4.77 (d, $J = 12.0$ Hz, 1H), 4.72 (d, $J = 10.9$ Hz, 1H), 4.62 (d, $J = 12.0$ Hz, 1H), 4.55 (d, $J = 3.4$ Hz, 1H), 4.52 (d, $J = 2.4$ Hz, 1H), 4.47 (dd, $J = 6.1, 14.2$ Hz, 1H), 4.00 (t, $J = 9.2$ Hz, 1H), 3.93 (br m, 1H), 3.42 (dd, $J = 3.4, 9.6$ Hz, 1H), 3.18 (s, 3H), 3.14 (t, $J = 9.4$ Hz, 1H), 3.29 (t, $J = 7.6$ Hz, 2H), 1.59 (br m, 2H), 1.25 (br s, 24H), 0.88 (t, $J = 6.7$ Hz, 3H); ^{13}C NMR (100 MHz, CDCl_3): δ 173.4, 142.7, 138.2, 137.8, 128.3, 128.3, 128.3, 128.0, 127.8, 127.8, 127.6, 125.0, 97.9, 81.7, 79.8, 77.8, 75.6, 74.8, 73.3, 68.9, 57.3, 55.1, 50.5, 34.0, 31.8, 29.5, 29.5, 29.4, 29.3, 29.2, 29.1, 29.0, 24.7, 22.5, 14.0; LRESIMS: m/z calcd for $[\text{C}_{47}\text{H}_{65}\text{N}_3\text{O}_7 + \text{H}]^+$: 784.5, found: 784.4.

4.2.2. Methyl 2,3,4-tri-*O*-benzyl-6-deoxy-6-(1'*H*-1',2',3'-triazolyl-4-yl-hexadecanoate)- α -*D*-galactopyranoside (**7**)

From compound **4** (226 mg, 0.462 mmol) and **5** (271.6 mg, 0.923 mmol), column chromatography (petroleum ether–EtOAc, 8:1→3:1) afforded **7** as a white ceraceous solid (347.5 mg, 96.0%). TLC: $R_f = 0.24$ (petroleum ether–EtOAc, 3:1); $[\alpha]_D^{25} +37.1$ (c 0.2, CH_2Cl_2); ^1H NMR (400 MHz, CDCl_3): δ 7.52 (s, 1H), 7.42–7.29 (br m, 15H), 5.15 (s, 2H), 5.04 (d, $J = 11.5$ Hz, 1H), 4.91 (d, $J = 11.7$ Hz, 1H), 4.84 (d, $J = 12.0$ Hz, 1H), 4.76 (d, $J = 11.9$ Hz, 1H), 4.68 (d, $J = 12.0$ Hz, 1H), 4.63 (d, $J = 11.5$ Hz, 1H), 4.60 (d, $J = 3.4$ Hz, 1H), 4.32 (dd, $J = 9.3, 14.0$ Hz, 1H), 4.19 (dd, $J = 3.0, 14.0$ Hz, 1H), 4.03 (dd, $J = 3.6, 10.0$ Hz, 1H), 3.99 (br dd, $J = 2.3, 9.4$ Hz, 1H), 3.93 (dd, $J = 2.5, 10.2$ Hz, 1H), 3.84 (br s, 1H), 2.98 (s, 3H), 2.27 (t, $J = 7.7$ Hz, 2H), 1.57 (m, 2H), 1.25 (br s, 24H), 0.88 (t, $J = 6.7$ Hz, 3H); ^{13}C NMR (100 MHz, CDCl_3): δ 173.2, 142.5, 138.2, 138.0, 137.7, 128.4, 128.3, 128.2, 128.1, 127.9, 127.8, 127.6, 127.5, 127.4, 124.8, 98.5, 78.5, 75.9, 74.8, 74.4, 73.6, 73.4, 69.2, 57.1, 54.9, 51.0, 33.8, 31.7, 29.4, 29.4, 29.3, 29.2, 29.1, 29.0, 28.8, 24.6, 22.4, 13.9.

4.3. General procedure for debenzylation

To a solution of benzylated glycolipids in MeOH (8–16 mL) was added PdCl_2 (0.5 equiv) and such mixture was stirred vigorously under hydrogen atmosphere for 20 min. The hydrogen gas was released rapidly and the mixture system was refilled with H_2 and stirred for another 20 min. The resulting mixture was then filtered

and concentrated under reduced pressure to give the crude residue which was purified by column chromatography.

4.3.1. Methyl 6-deoxy-6-(1'H-1',2',3'-triazolyl-4-yl-hexadecanoate)- α -D-glucopyranoside (8)

From compound **6** (265 mg, 0.338 mmol), column chromatography (EtOAc–EtOH, 12:1→8:1) afforded **8** as a white solid (135.1 mg, 77.8%). TLC: R_f = 0.66 (EtOAc–MeOH, 6:1); $[\alpha]_D^{+49.2}$ (c 0.2, CH₃OH); ¹H NMR (400 MHz, CDCl₃): δ 7.76 (s, 1H), 5.20 (s, 2H), 4.71 (br s, 2H), 4.63 (br d, J = 13.8 Hz, 1H), 3.89 (br s, 1H), 3.74 (t, J = 8.7 Hz, 1H), 3.42 (br d, J = 7.8 Hz, 1H), 3.24 (s, 3H), 3.12 (t, J = 8.7 Hz, 1H), 2.30 (t, J = 7.5 Hz, 2H), 1.59 (m, 2H), 1.25 (br s, 24H), 0.88 (t, J = 6.6 Hz, 3H); ¹³C NMR (100 MHz, CDCl₃): δ 173.5, 142.7, 125.7, 99.5, 73.6, 71.6, 70.7, 69.9, 57.2, 55.2, 50.8, 34.0, 31.8, 29.6, 29.6, 29.5, 29.4, 29.2, 29.2, 29.0, 24.7, 22.6, 14.0; HRESIMS: m/z calcd for [C₂₆H₄₇N₃O₇+H]⁺: 514.3492, found: 514.3489.

4.3.2. Methyl 6-deoxy-6-(1'H-1',2',3'-triazolyl-4-yl-hexadecanoate)- α -D-galactopyranoside (9)

From compound **7** (280 mg, 0.357 mmol), column chromatography (EtOAc–EtOH, 12:1→8:1) afforded **9** as a white solid (143.7 mg, 78.4%). TLC: R_f = 0.46 (EtOAc–MeOH, 6:1); $[\alpha]_D^{+50.1}$ (c 0.1, CH₃OH); ¹H NMR (400 MHz, CDCl₃): δ 7.72 (s, 1H), 5.21 (s, 2H), 4.78 (d, J = 3.3 Hz, 1H), 4.68 (dd, J = 4.5, 14.4 Hz, 1H), 4.59 (dd, J = 8.8, 14.4 Hz, 1H), 4.16 (br dd, J = 5.5, 8.2 Hz, 1H), 3.93 (br s, 1H), 3.82 (br dd, J = 3.8, 10.4 Hz, 1H), 3.78 (br dd, J = 2.9, 9.2 Hz, 1H), 3.17 (s, 3H), 2.30 (t, J = 7.5 Hz, 2H), 1.59 (m, 2H), 1.25 (br s, 24H), 0.88 (t, J = 6.7 Hz, 3H); ¹³C NMR (100 MHz, CDCl₃+CD₃OD): δ 173.4, 142.0, 125.0, 99.5, 69.4, 69.2, 68.8, 68.1, 56.4, 54.1, 50.7, 33.3, 31.2, 28.9, 28.9, 28.8, 28.7, 28.6, 28.5, 28.3, 24.1, 21.9, 13.0; HRESIMS: m/z calcd for [C₂₆H₄₇N₃O₇+H]⁺: 514.3492, found: 514.3482.

4.4. π -A isotherm measurement

The π -A isotherms of glycolipid monolayers were measured by using a model 612D computerized Langmuir film balance (Nima Technology, Coventry, UK). The spreading solution was prepared by dissolving glycolipids into chloroform with a concentration of 1 mg/ml. Then, 70 μ L of the solution was spread on pure MilliQ water (HPLC grade) surface and 10 min was allowed for solvent evaporation. The rectangular polytetrafluoroethylene PTFE trough (20 \times 30 cm²) having two movable barriers was filled with water. The temperature of the subphase was maintained at 25 \pm 0.1 $^{\circ}$ C by circulatory water from a thermostat circulated trough during experiment. In order to clear up the contaminant, a PTFE nozzle with an aspirator pump connected was applied to suck the surface of the subphase before experiments. The compression rate used in the study was 10 cm/min. The overall reproducibility in different runs was ensured by 5–6 times measurements for each sample.

4.5. LB films transfer

Glycolipids or PDA-glycolipid films were transferred by using Langmuir–Blodgett (LB) technique at various surface pressures in the range of 5–35 mN/m. The experiment was performed by pulling the mica up vertically from the Langmuir trough. Freshly cleaved mica was immersed in the subphase before spreading the glycolipid solution.

4.6. Measurement of water contact angle

The values of water contact angle θ of different LB films were measured by a sessile drop method at 25 $^{\circ}$ C using an image analysis (custom built equipment provided by Zhongchen Instrument

Co., China). The volume of MilliQ water droplet was 0.5 μ L. The θ value of mica is nearly zero.

4.7. Observation of surface morphology

The morphology of glycolipid LB films on mica was obtained by using AFM (AJ-III, Aijian nanotechnology Inc., China) in air with a tapping mode at room temperature. The cantilever of AFM tip was (Mikro Masch Co., Russia) a Si pyramidal tip with a spring constant of 3.0 N/m. All images were obtained at least five macroscopically separated areas and were analyzed off-line by using the software provided with the AFM instruments.

Acknowledgments

This work was financial supported by National Natural Science Foundation of China (Grant Nos. 20876045 and 21076071), Shanghai Science and Technology Community (No. 10410702700) and the Fundamental Research Funds for the Central Universities (No. WK1013002). X.-P. He also gratefully acknowledges the French Embassy for the financial support of a co-tutored doctoral program.

Supplementary data

Supplementary data associated with this article can be found, in the online version, at doi:10.1016/j.carres.2011.04.038.

References

- Tsuji, M. *Cell Mol. Life Sci.* **2006**, *63*, 1889–1898.
- Wu, D.; Fujio, M.; Wong, C.-H. *Bioorg. Med. Chem.* **2008**, *16*, 1073–1083.
- Worakitkanchanakul, W.; Imura, T.; Fukuoka, T.; Morita, T.; Sakai, H.; Abe, M.; Rujiravanit, R.; Chavadej, S.; Minamikawae, H.; Kitamoto, D. *Colloids Surf., B* **2008**, *65*, 106–112.
- Morita, T.; Fukuoka, T.; Konishi, M.; Imura, T.; Yamamoto, S.; Kitagawa, M.; Sogabe, A.; Kitamoto, D. *Appl. Microbiol. Biotechnol.* **2009**, *83*, 1017–1025.
- Piazza, M.; Rossini, C.; Fiorentina, S. D.; Pozzi, C.; Comelli, F.; Bettoni, I.; Fusi, P.; Costa, B.; Peri, F. *J. Med. Chem.* **2009**, *52*, 1209–1213.
- Li, K.; Ichikawa, S.; Al-Dabbagh, B.; Bouhss, A.; Matsuda, A. *J. Med. Chem.* **2010**, *53*, 3793–3813.
- Zhang, Z.; Zong, C.; Song, G.; Lv, G.; Chun, Y.; Wang, P.; Ding, N.; Li, Y. *Carbohydr. Res.* **2010**, *345*, 750–760.
- Vogel, J.; Bendas, G.; Bakowsky, U.; Hummel, G.; Schimidt, R. R.; Ketmann, U.; Rothe, U. *Biochim. Biophys. Acta* **1998**, *1372*, 205–215.
- Falconer, R. A.; Toth, I. *Bioorg. Med. Chem.* **2007**, *15*, 7012–7020.
- de Almeida, M. V.; Hyaric, M. L. *Mini-Rev. Org. Chem.* **2005**, *2*, 283–297.
- Thiesen, P. H.; Rosenfeld, H.; Konidala, P.; Garamus, V. M.; He, L.; Prange, A.; Niemeyer, B. *J. Biotechnol.* **2006**, *124*, 284–301.
- Kolb, H. C.; Finn, M. G.; Sharpless, K. B. *Angew. Chem., Int. Ed.* **2001**, *40*, 2004–2021.
- Rostovtsev, V. V.; Green, L. G.; Fokin, V. V.; Sharpless, K. B. *Angew. Chem., Int. Ed.* **2002**, *41*, 2596–2599.
- Aragão-Leoneti, V.; Campo, V. L.; Gomes, A. S.; Field, R. A.; Carvalho, I. *Tetrahedron* **2010**, *66*, 9475–9492.
- Fu, Q.; Liang, T.; Zhang, X.; Du, Y.; Guo, Z.; Liang, X. *Carbohydr. Res.* **2010**, *345*, 2690–2697.
- Kumar, K. K.; Kumar, R. M.; Subramanian, V.; Das, T. M. *Carbohydr. Res.* **2010**, *345*, 2297–2304.
- Dedola, S.; Hughes, D. L.; Nepogodiev, S. A.; Rejzek, M.; Field, R. A. *Carbohydr. Res.* **2010**, *345*, 1123–1134.
- Koschella, A.; Richter, M.; Heinze, T. *Carbohydr. Res.* **2010**, *345*, 1028–1033.
- Chen, Y.-B.; Wang, Y.-J.; Lin, Y.-J.; Hu, C.-H.; Chen, S. J.; Chir, J. L.; Wu, A. T. *Carbohydr. Res.* **2010**, *345*, 956–959.
- Zhang, L.; Wei, G.; Du, Y. *Carbohydr. Res.* **2009**, *344*, 2083–2087.
- Cheng, K.; Liu, J.; Liu, X.; Li, H.; Sun, H.; Xie, J. *Carbohydr. Res.* **2009**, *344*, 841–850.
- Maschauer, S.; Prante, O. *Carbohydr. Res.* **2009**, *344*, 753–761.
- Yeoh, K. K.; Butters, T. D.; Wilkinson, B. L.; Fairbanks, A. J. *Carbohydr. Res.* **2009**, *344*, 586–591.
- Mallard-Favier, I.; Blach, P.; Cazier, F.; Delattre, F. *Carbohydr. Res.* **2009**, *344*, 161–166.
- Song, Z.; He, X. P.; Li, C.; Gao, L. X.; Wang, Z. X.; Tang, Y.; Xie, J.; Li, J.; Chen, G.-R. *Carbohydr. Res.* **2011**, *346*, 140–145.
- Lin, L.; Shen, Q.; Chen, G.-R.; Juan, X. *Bioorg. Med. Chem.* **2008**, *16*, 9757–9763.
- Zhang, Y.-J.; He, X.-P.; Li, C.; Li, Z.; Shi, D.-T.; Gao, L. X.; Qiu, B. Y.; Shi, X. X.; Tang, Y.; Li, J.; Chen, G. R. *Chem. Lett.* **2010**, *39*, 1261–1263.
- Yang, J.-W.; He, X.-P.; Zhao, H.; Gao, L.-X.; Zhang, W.; Shi, X.-X.; Tang, Y.; Li, J.; Chen, G. R. *Bull. Korean Chem. Soc.* **2010**, *31*, 3359–3365.

29. Paul, K. J. V.; Loganathan, D. *Tetrahedron Lett.* **2008**, *49*, 6356–6359.
30. Neto, V.; Granet, R.; Krausz, P. *Tetrahedron* **2010**, *66*, 4633–4646.
31. Guillemineau, M.; Singh, S.; Grossutti, M.; Auzanneau, F. I. *Carbohydr. Res.* **2010**, *345*, 2723–2730.
32. Song, S. X.; Zhang, H. L.; Kim, C. G.; Sheng, L.; He, X. P.; Long, Y. T.; Li, J.; Chen, G. R. *Tetrahedron* **2010**, *66*, 9974–9980.
33. Kobertz, W. R.; Bertozzi, C. R.; Bednarski, M. D. *J. Org. Chem.* **1996**, *61*, 1894–1897.
34. Li, S. C.; Meng, X. B.; Cai, M.-S.; Li, Z. J. *Synth. Commun.* **2006**, *36*, 637–643.
35. Chen, Q.; Liang, X.; Wang, S.; Xu, S.; Liu, H.; Hu, Y. *J. Colloid Interf. Sci.* **2007**, *314*, 651–658.
36. Truzzolillo, D.; Bordi, F.; Cametti, C.; Sennato, S. *Colloids Surf., A* **2008**, *319*, 51–61.
37. Zhang, G.; Marie, P.; Maaloum, M.; Muller, P.; Benoit, N.; Krafft, M. P. *J. Am. Chem. Soc.* **2005**, *127*, 10412–10419.
38. Yu, Z. W.; Jin, J.; Cao, Y. *Langmuir* **2002**, *18*, 4530–4531.
39. Minones, J., Jr.; Pais, S.; Minones, J.; Conde, O.; Dynarowicz-Latka, P. *Biophys. Chem.* **2009**, *140*, 69–77.
40. Sarkar, R.; Pal, P.; Mahato, M.; Kamilya, T.; Chaudhuri, A.; Talapatra, G. B. *Colloids Surf., B* **2010**, *79*, 384–389.
41. Sergi, G. M.; Oscar, D.; OmèFausto, S.; Teresa, M.; Jordi, H.-B. *Biochim. Biophys. Acta* **2007**, *1768*, 1190–1198.
42. Zhang, Y.; Cheng, X.; Wang, J. X.; Zhou, F. M. *Colloids Surf., A* **2009**, *337*, 26–32.
43. Xu, S.; Liu, A.; Chen, Q.; Lv, M.; Yonese, M.; Liu, H. *Colloids Surf., B* **2009**, *70*, 124–131.
44. Boullanger, P.; Lafont, D.; Bouchu, M. N.; Jiang, L.; Liu, T.; Lu, W.; Guo, C. X.; Li, J. *C. R. Chim.* **2008**, *11*, 43–60.
45. Deng, J.; Sheng, Z.; Zhou, K.; Duan, M.; Yu, C.-Y.; Jiang, L. *Bioconjugate Chem.* **2009**, *20*, 533–537.